Article

Programmable Fluidic Production of Microparticles with Configurable Anisotropy

Kyung Eun Sung, Siva A. Vanapalli, Deshpremy Mukhija, Hugh A. McKay, Joanna Mirecki Millunchick, Mark A. Burns, and Michael J. Solomon

J. Am. Chem. Soc., **2008**, 130 (4), 1335-1340 • DOI: 10.1021/ja0762700

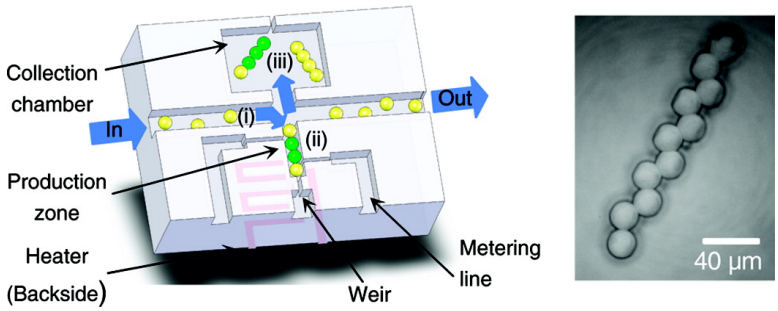

More About This Article

Additional resources and features associated with this article are available within the HTML version:

- Supporting Information
- Links to the 8 articles that cite this article, as of the time of this article download
- Access to high resolution figures
- Links to articles and content related to this article
- Copyright permission to reproduce figures and/or text from this article

View the Full Text HTML

J|A|C|S
ARTICLES
Published on Web 01/01/2008

Programmable Fluidic Production of Microparticles with Configurable Anisotropy

Kyung Eun Sung,[†] Siva A. Vanapalli,[†] Deshpremy Mukhija,[†] Hugh A. McKay,[‡] Joanna Mirecki Millunchick,[‡] Mark A. Burns,[†,§] and Michael J. Solomon*,[†]

Department of Chemical Engineering, Department of Materials Science and Engineering, Department of Biomedical Engineering, University of Michigan, Ann Arbor, Michigan

Received August 20, 2007; E-mail: mjsolo@umich.edu

Abstract: We report a technique for continuous production of microparticles of variable size with new forms of anisotropy including alternating bond angles, configurable patchiness, and uniform roughness. The sequence and shape of the anisotropic particles are configured by exploiting a combination of confinement effects and microfluidics to pack precursor colloids with different properties into a narrow, terminal channel. The width and length of the channel relative to the particle size fully specify the configuration of the anisotropic particle that will be produced. The precursor spheres packed in the production zone are then permanently bonded into particles by thermal fusing. The flow in the production zone is reversed to release the particles for collection and use. Particles produced have linear chain structure with precisely configured, repeatable bond angles. With software programmable microfluidics, sequence and shape anisotropy are combined to yield synthesized homogeneous (type "A"), surfactantlike (type "A−B") or triblock (type "A−B−A") internal sequences in a single device. By controlling the dimensions of the microfluidic production zone, triangular prisms and particles with controlled roughness and patchiness are produced. The fabrication method is performed with precursors spheres with diameter as small as 3.0 μm.

Introduction

Demand for particles with shape and interaction anisotropy is fueled by applications in self-assembly,[1,2] drug delivery carrier design,[3] and barcoding.[4] Subtle changes in particle anisotropy produce surprising effects. For example, transforming a rod from a spherocylinder to an ellipsoid eliminates its smectic phase, and the transition pressure of the liquid crystal cubatic phase is linked to cube roughness.[5,6] In addition, particle shape is a determinant of the efficacy of macrophage phagocytosis.[3] The richness of applications for anisotropic particles has driven research in new particle production techniques. Batch syntheses have yielded a broad array of faceted, branched, and patterned particles[1] including colloidal molecules[7,8] as well as patchy[9] and Janus[10] particles. Electrical, optical, magnetic, and deformation fields have also been applied to produce anisotropic colloidal particles.[11]

Uniformity of anisotropic particle shape and internal structure is critical to self-assemble complex structures and arrays for end-use applications such as photonic band gap materials.[12] Among the explosion of recent synthetic methods, two classes—those based on confinement effects and those based on microfluidics—yield exceptional uniformity. First, Xia and co-workers have formed colloidal molecules and chains by confinement of particles in patterned surfaces and channels,[8,13] while Wu and co-workers[14] have formed nonclose-packed lattices by self-assembly of millimeter-scale beads confined in

[†] Department of Chemical Engineering.
[‡] Department of Materials Science and Engineering.
[§] Department of Biomedical Engineering.

(1) Glotzer, S. C.; Solomon, M. J. *Nat. Mater.* **2007**, *6*, 557−562.
(2) Glotzer, S. C.; Solomon, M. J.; Kotov, N. A. *AIChE J.* **2004**, *50*, 2978−2985.
(3) Champion, J. A.; Mitragotri, S. *Proc. Natl. Acad. Sci. U.S.A.* **2006**, *103*, 4930−4934.
(4) Pregibon, D. C.; Toner, M.; Doyle, P. S. *Science* **2007**, *315*, 1393−1396.
(5) John, B. S.; Stroock, A.; Escobedo, F. A. *J. Chem Phys.* **2004**, *120*, 9383−9389.
(6) John, B. S.; Escobedo, F. A. *J. Phys. Chem B* **2005**, *109*, 23008−23015.
(7) Valignat, M. P.; Theodoly, O.; Crocker, J. C.; Russel, W. B.; Chaikin, P. M. *Proc. Natl. Acad. Sci. U.S.A.* **2005**, *102*, 4225−4229; Lu, Y.; Xiong, H.; Jiang, X. C.; Xia, Y. N.; Prentiss, M.; Whitesides, G. M. *J. Am. Chem. Soc.* **2003**, *125*, 12724−12725; Rolland, J. P.; Maynor, B. W.; Euliss, L. E.; Exner, A. E.; Denison, G. M.; DeSimone, J. M. *J. Am. Chem. Soc.* **2005**, *127*, 10096−10100; Hernandez, C. J.; Mason, T. G. *J. Phys. Chem.* C **2007**, *111*, 4477−4480; Manoharan, V. N.; Elsesser, M. T.; Pine, D. J. *Science* **2003**, *301*, 483−487; Cho, Y. S.; Yi, G. R.; Lim, J. M.; Kim, S. H.; Manoharan, V. N.; Pine, D. J.; Yang, S. M. *J. Am. Chem. Soc.* **2005**, *127*, 15968−15975.
(8) Yin, Y.; Lu, Y.; Gates, B.; Xia, Y. *J. Am. Chem. Soc.* **2001**, *2001*, 8718−8729.
(9) Zhang, G.; Wang, D. Y.; Mohwald, H. *Angew. Chem., Int. Ed.* **2005**, *44*, 7767−7770.
(10) Cayre, O.; Paunov, V. N.; Velev, O. D. *J. Mater. Chem.* **2003**, *13*, 2445−2450.
(11) Furst, E. M.; Suzuki, C.; Fermigier, M.; Gast, A. P. *Langmuir* **1998**, *14*, 7334−7336; Terray, A.; Oakey, J.; Marr, D. W. M. *Appl. Phys. Lett.* **2002**, *81*, 1555−1557; Roh, K. H.; Martin, D. C.; Lahann, J. *Nat. Mater.* **2005**, *4*, 759−763; Roh, K. H.; Martin, D. C.; Lahann, J. *J. Am. Chem. Soc.* **2006**, *128*, 6796−6797; Champion, J. A.; Katare, Y. K.; Mitragotri, S. *Proc. Natl. Acad. Sci. U.S.A.* **2007**, *104*, 11901−11904; Mohraz, A.; Solomon, M. J. *Langmuir* **2005**, *21*, 5298−5306.
(12) Ozin, G. *Chem Commun.* **2003**, 2639−2643.; Colvin, V. L. *MRS Bull.* **2001**, *26*, 637−641.
(13) Xia, Y.; Yin, Y.; Lu, Y.; McLellan, J. *Adv. Funct. Mater.* **2003**, *13*, 907−918; Yin, Y.; Xia, Y. *J. Am. Chem. Soc.* **2003**, *125*, 2048−2049.
(14) Wu, H. K.; Thalladi, V. R.; Whitesides, S.; Whitesides, G. M. *J. Am. Chem. Soc.* **2002**, *124*, 14495−14502.

packed columns. Second, microfluidic methods have introduced the possibility of continuous production. For example, two-phase flow through a microfabricated nozzle or T-junction yields droplets of controlled size that can be subsequently solidified into particles.[15] Alternatively, local regions of a monomer solution have been polymerized by flow-through photolithography.[16]

To date, confinement-based synthetic methods lack the continuous-processing capability of microfluidics including the potential for programmable operation. Meanwhile, the microfluidics methods, all based on the solidification of liquid precursors, lack the means to flexibly introduce complex internal shape and material anisotropy. Combining the attributes of confinement and microfluidics in a single fabrication method would yield the ability to simultaneously program highly uniform shape and material sequences into the particles. Such a flexible method could be applied to continuously produce particles with classes of anisotropy that are not available through either approach, or by any other method.

Here we introduce such a continuous fabrication technique based on the principles of confinement, microfluidic processing, and permanent bonding to yield particles with novel and configurable forms of shape and material anisotropy. In addition to possessing global shape anisotropy, these particles also incorporate new forms of local anisotropy, including repeated bond angles, concavity, and uniform roughness. With software programmable microfluidics, the material anisotropy of linear chains can be designed to yield homogeneous (type "A"), surfactantlike (type "A−B") or tri-block (type "A−B−A") internal sequences—all produced in a single device. Moreover, the continuous fluid processing method makes only minimal constraints on the input precursor particles. Thus, although here we use latex beads with different optical signatures to distinguish between types "A" and "B", the rich array of materials and chemistries that have been previously incorporated into microparticles are equally well compatible with the method. Because of the method's programmability and the unique way in which shape and material anisotropy are combined, anisotropic particles produced by it will be applicable to areas of the chemical sciences such as barcoding,[17] self-assembly,[18] and drug delivery carrier design.[3]

Results and Discussion

Fabrication Concept, Design, and Operation. In our approach (Figure 1A), programmable fluid flow is used to sequentially transport precursor particles through a series of narrow (i.e., approximately one particle diameter in width and depth) channels. A constriction or weir in the channel collects the particle sequence with programmed anisotropy in the production zone. A variety of techniques can be used to bond the anisotropic assembly including sintering, UV-initiated photopolymerization, carboxyl amine chemistry, DNA hybridization, or receptor−ligand binding. After bonding, the flow is reversed to release the manufactured particle for collection and use. A key feature of this scheme is that metering lines located along the production zone allow the internal (material) sequence of the particle chain to be specified by means of a series of software-programmed pressure actuation steps. For example, each of the material sequences (products) shown at Figure 1A, right, can be made by means of the two-metering line device.

Figure 1B reports the steps of a typical production cycle. The particle produced is a linear chain of homogeneous sequence with regular, alternating bond angles. The geometry of the production zone fixes both the length ($N = 11$) and bond angle (angle relative to particle centerline, $\alpha = 29.3° \pm 2.3°$). Continuous flow ($Q \approx 3.5\ \mu$L/min) through the production zone compresses the sequence. An on-chip resistive heater raises the local temperature to near the glass transition point to fuse the particles into a permanently bonded chain. The minimum time for fusing is 300 ms. The high-resolution optical micrograph shows that the alternating structure created by the fluidic processing is conserved during the fusing step.

One unexpected effect of applying vacuum pressure to the weir during the thermal profile, as shown in the Figure 1B micrograph, is that the shape of the weir is imprinted on the tail of the synthesized chain. This imprint uniquely identifies a particle's head and tail, thereby approximately doubling the amount of information that could be encoded in their anisotropic structure for applications such as colloidal barcoding.[3] If desired, actuating the weir pressure profile during the production step removes the shape effect (as shown, e.g., for chains in Figure 4).

Figure 2 describes how pressure inputs to the device are used to control the loading, washing, fusing, and release steps in each fabrication cycle. Pressure is actuated among three states including high-, neutral-, and low-pressure settings at seven channels. We note that the wash step is included in every fabrication cycle to avoid or remove defective assemblies prior to the fusion step.

The duration of each step discussed in Figure 2 is configured according to the number of precursor spheres incorporated into the anisotropic particle. For example, we find the production rate (turnover frequency) of a 5-particle anisotropic chain is 0.29 Hz. For a 10-particle chain, the production rate was 0.17 Hz. For a 20-particle chain, the rate was measured to be 0.06 Hz. The longest-duration operation in these (unoptimized) production cycles is the loading step. In particular, because particle concentrations in the device channels are low (∼0.05 wt %), the time required to assemble the unbonded sequence consumes about half the cycle time. The loading time also increases with chain length, because of the greater time required to pack the longer particle sequences.

Production Uniformity. An effect of the thermal profile is to flatten the sides of the particles that compose the chain, as shown in Figure 1B (iv). This flattening is due to slight distortion of the particles by the microchannel walls as they are softened during fusing. While this nonsphericity may be desirable for some applications, the amount of distortion can be controlled or eliminated by adjusting the fusion temperature. Figure 3 reports the effect of the fusion temperature on the sphericity of the particles that are incorporated into the particle chains. We

(15) Nie, Z. H.; Xu, S. Q.; Seo, M.; Lewis, P. C.; Kumacheva, E. *J. Am. Chem. Soc.* **2005**, *127*, 8058−8063; Nisisako, T.; Torii, T.; Higuchi, T. *Chem. Eng. J.* **2004**, *101*, 23−29; Fernandez-Nieves, A.; Cristobal, G.; Garces-Chavez, V.; Spalding, G. C.; Dholakia, K.; Weitz, D. A. *Adv. Mater.* **2005**, *17*, 680; Shepherd, R. F.; Conrad, J. C.; Rhodes, S. K.; Link, D. R.; Marquez, M.; Weitz, D. A.; Lewis, J. A. *Langmuir* **2006**, *22*, 8618−8622; Dendukuri, D.; Tsoi, K.; Hatton, T. A.; Doyle, P. S. *Langmuir* **2005**, *21*, 2113−2116.
(16) Dendukuri, D.; Pregibon, D. C.; Collins, J.; Hatton, T. A.; Doyle, P. S. *Nat. Mater.* **2006**, *5*, 365−369.
(17) Braeckmans, K.; De Smedt, S. C.; Leblans, M.; Pauwels, R.; Demeester, J. *Nat. Rev. Drug Discovery* **2002**, *1*, 447−456.
(18) Anderson, V. J.; Lekkerkerker, H. N. W. *Nature* **2002**, *416*, 811−815; Ozin, G. A.; Arsenault, A. C. *Nanochemistry: A Chemical Approach to Nanomaterials*; Royal Society of Chemistry: Cambridge, 2005.

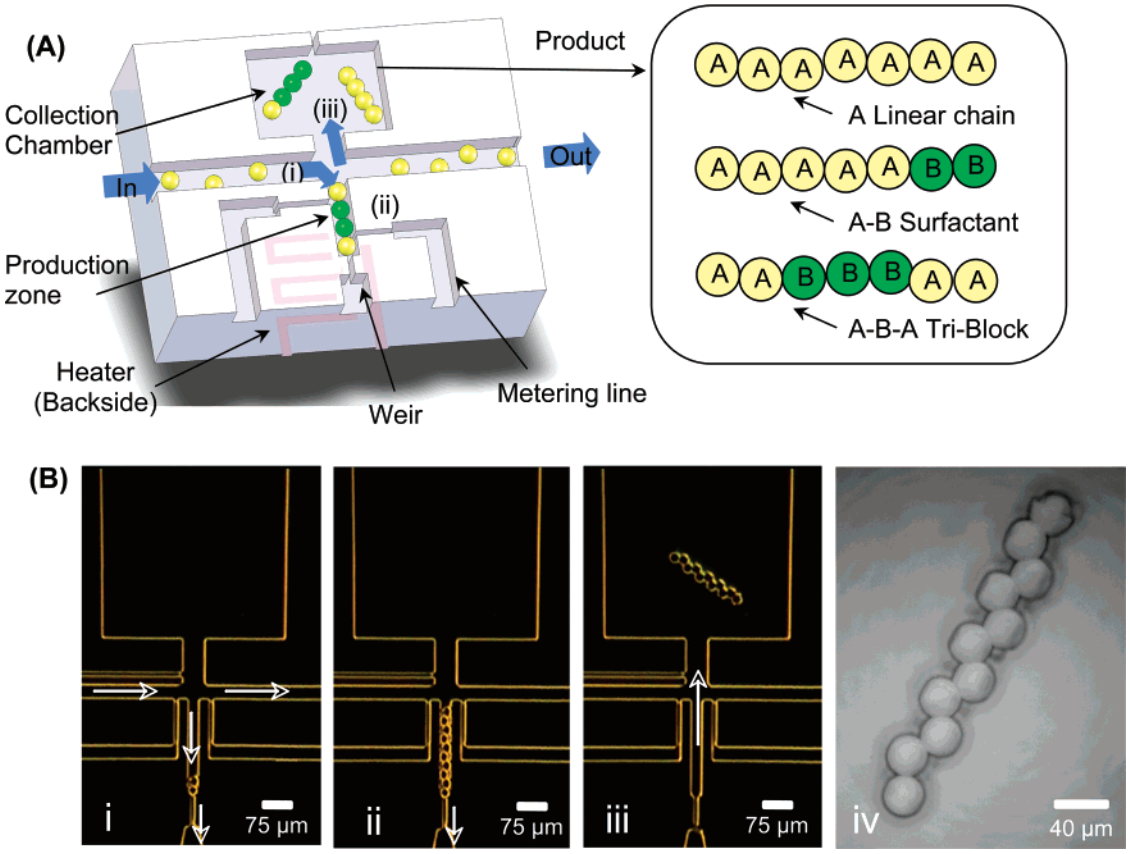

Figure 1. (A) Schematic diagram of the continuous fabrication process. Particles (0.05 wt %) flow single-file in DMSO to the production zone (i) where they undergo reaction (ii) and collection (iii). The length and width of the zone and the actuation of input and metering lines control the sequence synthesized. Depending on actuation, each of three kinds of chains shown can be synthesized. **(**B**)** Image sequence shows the operational steps involved in the fabrication of a particle chain by thermal fusing. The sequence is loaded (i), fused (ii), and released (iii). Arrows show direction of flow. The input particles are 21.1 μm polystyrene beads. Fusing is accomplished at $T = 80$ °C by operating a Ti/Pt heater fabricated on the back of the chip. After heating, the particle is cooled by convective flow and then released into the collection chamber. (iv) High-resolution optical microscopy image of the particle chain synthesized. The tail of the particle has been imprinted with the geometry of the flow constriction at the end of the production zone. The sphericity of the particles in the chain is a function of the fusing temperature.

ii	Inject	Wash	Heat	Eject
1	P	N	N	N
2	N	P	N	P
3	V	V	V	P
4	N	N	N	P
5	N	V	N	N
6	P	P	P	N
7	N	N	N	V

- P : Pressure (≈ 8 psi)
- N : Neutral
- V : Vacuum (≈ 10 inHgVac)

Figure 2. Typical operation cycle to produce the anisotropic particle shown in Figure 1. Seven channels (numbered as in left panel) are actuated among three states (positive pressure, positive vacuum, neutral) to load precursor spheres, wash/meter the sequence of particles packed at the weir, fuse the packed sequence, and eject it into the product reservoir.

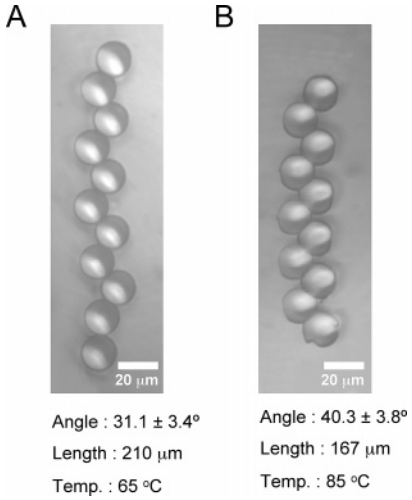

Figure 3. Effect of fusing temperature on the sphericity of particles configured into anisotropic chains. As the fusing temperature is increased from 65 °C (A) to 85 °C (B) particles in the chain increasingly soften and distort along the microchannel wall of the production zone. The sphericity of the particles is greater at the lower set point fusing temperature than at the higher set point.

find that during fusing the particles may flatten against the microchannel walls. The degree of distortion is principally controlled by the fusing temperature. At low fusing temperatures ($T = 65$ °C), the particles soften to only a small degree. In this case, the distortion effects are minimal, and the sphericity of the particles of the chain is very high (Figure 3A). At high fusing temperatures ($T = 85$ °C), the particles are more nonspherical

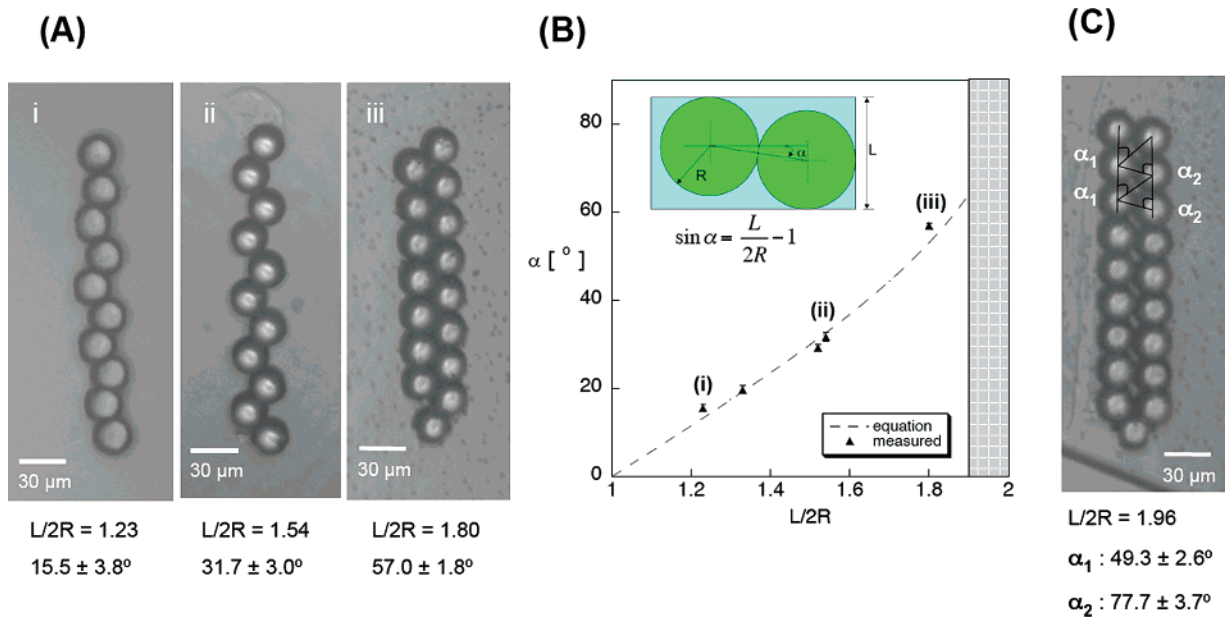

Figure 4. Effect of channel geometry on chain bond angle. **(**A**)** Image of synthesized particles chains with different bond angles. The interior bond angles of the permanent chains from image processing are shown. The number of monomers in each chain is consistent with the production zone geometry (i.e., width and length) used to produce it. **(**B**)** Comparison of experimental and theoretical bond angles. Error bars (standard error of the mean) are comparable to the size of the datum points. A regime in which chains with irregular bond angles are formed is shaded at the right of the plot. **(**C**)** Chain with irregular bond angles formed in a microchannel of dimensionless width $L/2R = 1.96$. The two (alternating) bond angles are 49.3 ± 2.5° and 77.7 ± 3.7°.

(Figure 3B). Thus, the sphericity of the particles in the chains can be controlled by adjusting the fusing temperature.

To evaluate the uniformity of the fabrication from particle to particle, we performed the following experiment and analysis: In a particular production run, a series of 26 chains, each 5 particles in length, was sequentially synthesized (i.e., yield = 100%). Of the chains, eight were randomly selected for high-resolution microscopy and bond angle analysis (cf. Experimental Section). The chains are highly uniform: the measured mean bond angle $\alpha = 32.4°$ with standard deviation, $\sigma = 1.5°$. In addition, the silicon devices did not fail due to jamming, clogging, or fouling during the loading, fusing, or release phases of the production cycle. For example, to date, multiple devices have been exercised for hundreds of production cycles without observing such effects. Thus, the process reproducibly yields highly uniform particles with a low failure rate. Design features that contribute to performance include: (i) dilute concentration of input particles (~0.05 wt %) to eliminate jamming; (ii) silicon substrate to minimize device/particle adhesion; (iii) metering (wash) lines to achieve additional fluidic flexibility and control. In particular, we use a wash step in every production cycle (cf. Figure 2) to remove excess particles from the top of the production zone and thereby avoid fusing defective assemblies.

Design and Control of Anisotropic Particle Internal Structure. This method is a powerful means to configure the shape and sequence of anisotropic particles. Because the ratio of channel width to particle diameter controls the bond and torsional angles between precursor particles, chain structure is reminiscent of polymers and can be varied from linear to alternating to helical.[19,20] Such corrugated chains also have local concavity potentially beneficial to drug delivery carrier design.[3] In the size range of interest here, a simple 2D model for the stacking of individual particles of radius R in a channel of width L is $\sin \alpha = L/2R - 1$, where α is the angle of a segment connecting the centroids of two adjacent particles relative to the centerline of the chain.[19] As shown in Figure 4A, we varied the ratio L/R to produce chains with α varying from 15.5 ± 3.8° to 57.0 ± 1.8°. Here the error is the standard deviation, σ, of all interior bond angles of the chain. The agreement between the bond angle model and the measured average is good, as shown in Figure 4B. As the bond angle is increased above ~60°, synthesized chains transition from a regular structure with a unique bond angle to an irregular one characterized by two bond angles (Figure 4C), again in good agreement with previous studies of sphere packings.[19] These results show that the precise control of chain structure yielded by microfabrication and fluidic processing propagates through the fusing step to the finished products.

We note that the interior bonds angles of the chains are very precise—the typical standard deviation of angles in a chain is less than 10% of the mean value, particularly for particles that are fused such that their sphericity is preserved (cf. Figure 3). In this case, the principle determinants of the variability in bond angles are the size polydispersity of the precusor spheres (σ = 3.5%) and the variation in the width of the microchannel production zone (σ = 0.6%).

Combining Material and Shape Anisotropy. In Figure 5 we show that the method's combination of local shape control and configurable sequence can be applied to synthesize permanently bonded particles with new kinds of anisotropy. As an example of programmed fluidic production, the top image sequence reports particles produced in a production zone configured with two metering lines. By coupling the sequential actuation of these lines with the input flow of either A or B particles, we produce A−B (Figure 5B) and A−B−A (Figure 5C) type sequence anisotropy. The particles are reminiscent of molecular agents for assembly such as surfactants, associative

(19) Kumacheva, E.; Garstecki, P.; Wu, H.; Whitesides, G. M. *Phys. Rev. Lett.* **2003**, *91*, 128301.
(20) Pickett, G. T.; Gross, M.; Okuyama, H. *Phys. Rev. Lett.* **2000**, *85*, 3652−3655.

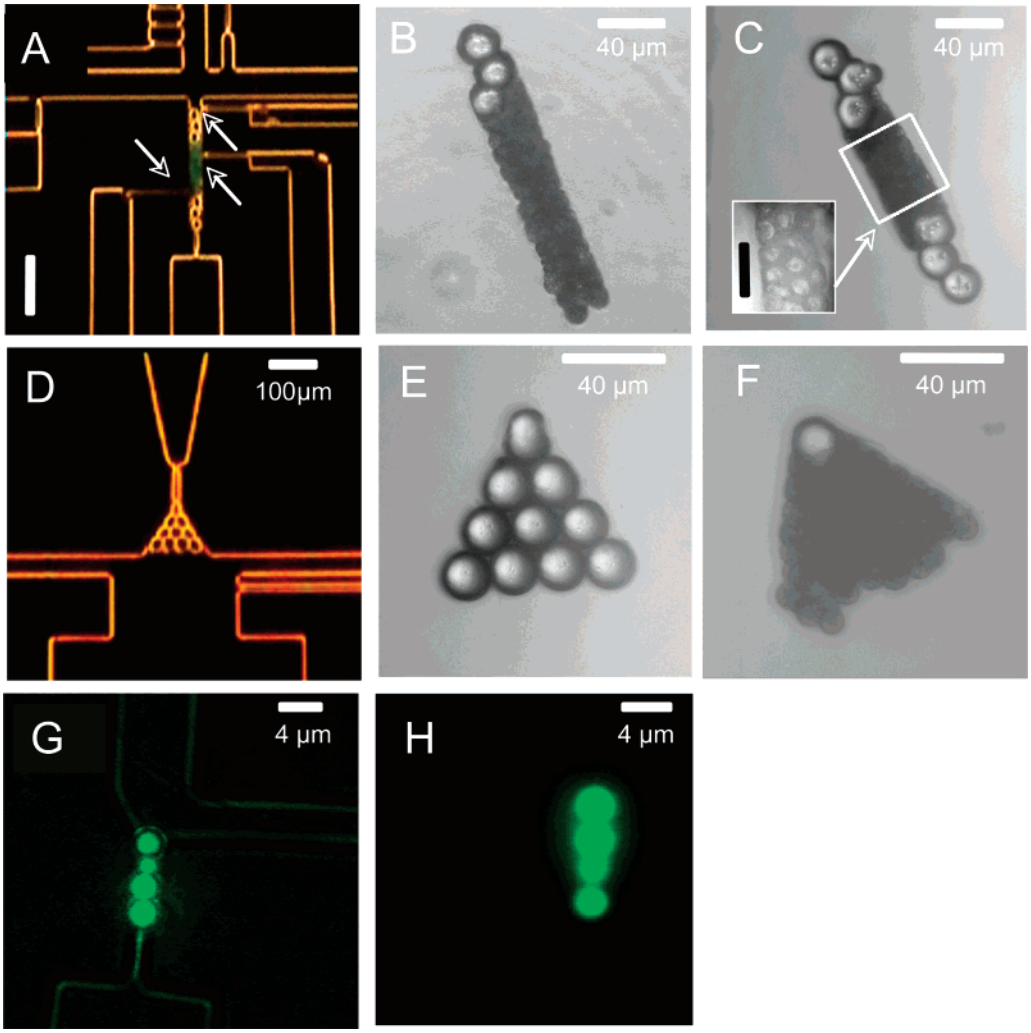

Figure 5. Material and shape anisotropy produced by the method. **(**A**)** Image of the production zone of a device configured with two metering lines for sequence control. The scale bar is 100 μm. The arrows indicate metering lines. The device can be used to produce types A, A−B, and A−B−A chains. The large (type-A) and small (type-B) polystyrene particle sizes are 21.1 and 9.9 μm, respectively. The small particles contain a blue dye to distinguish them. The A−B−A particle sequence shown is formed by repetition of the following cycle at each metering location: First, particles of appropriate type (A or B) are packed into the channel. Second, excess particles are expelled by actuation of the metering line. From this single-device design, chains with the material sequence heterogeneity of (B) and (C) are produced. The inset of Figure 3C is a high-resolution image showing that the internal structure of the small particles persists after fusing. The scale bar is 20 μm. The tapered channel production zone of (D) can be packed to form homogeneous triangular prisms with uniform roughness (E). Combining types A and B particles results in both shape anisotropy and patchiness (F). The size scalability of the method is shown in (G). FITC-labeled spheres of 3.0 μm diameter are packed in a production zone of depth 8.5 μm. The fused chain after release from the production zone is shown in (H). The variable fluorescence records the alternating bond angles that result from vertical packing in the production zone microchannel.

thickeners, and block copolymers. These microscale materials however display structural rigidity that is absent from their molecular analogues. Also in Figure 5, at bottom, we find that shape and material anisotropy can be combined to form particles with well-defined patchiness.[1] To form triangular prisms,[21] we taper the geometry of the production zone. The particles formed, shown in Figure 5E, display uniform roughness useful for tuning liquid-crystal phase boundaries.[6] In Figure 5F, we controllably introduce patchiness by labeling one vertex of the prism with a type A-particle. The remainder of the prism, populated with ~10-μm particles, shows roughness that differs from the particle formed from the ~20-μm spheres.

Anisotropic Particle Production from 3 μm Precursor Spheres. Applications of anisotropic particles exist on a variety of length scales. For example, while single-particle applications such as barcoding and drug delivery can be executed with microparticles, applications involving multiple particles, such as self-assembly, will proceed best on the micrometer scale. To evaluate this possibility, we produced anisotropic particles from fluorescent spheres of diameter 3.0 μm, about an order of magnitude smaller than particles used in Figure 4. This production required scale down of component technologies of microfabrication, fusing,[22,23] and particle convection in microchannels. Precursor spheres were fluidically convected to and assembled in the production zone (Figure 5G), thermally fused, and then ejected from the channel for fluorescence visualization (Figure 5H).

The Figure 5 panels shows that smaller particles can be incorporated into the production method in one of two ways. First, if the particle size is decreased at fixed channel size, the

(21) Malikova, N.; Pastoriza-Santos, I.; Schierhorn, M.; Kotov, N. A.; Liz-Marzan, L. M. *Langmuir* **2002**, *18*, 3694−3697.

(22) Mazur, S.; Beckerbauer, R.; Buckholz, J. *Langmuir* **1997**, *13*, 4287−4294.
(23) Yake, A. M.; Panella, R. A.; Snyder, C. E.; Velego, D. *Langmuir* **2006**, *22*, 9135.

anisotropic particles produced have greater fine structure with applications to, for example, roughness control. However, as discussed in ref 19 and as is apparent in Figure 5C, as the size is progressively decreased, the packing quality deteriorates. Second, as reported in Figure 5G,H, anisotropic particles with high-quality internal structure can be made from smaller particles if the channel dimension is decreased proportionally, thereby maintaining particle to channel size ratios characteristic of the results of Figure 4.

Conclusion

A powerful attribute of the method presented is that the particle's sequence can be dynamically controlled through fluidic processing. For instance, mixtures of types A, A−B, and A−B−A structures could all be made in a single linear channel device with the final composition of the mixture controlled solely by software. Parallelization of the channels in a single device offers further possibilities for enhanced synthetic flexibility and throughput. For example, the 1.08×0.66 mm^2 single-channel device of Figure 1B currently operates at rates up to about 0.25 Hz for the production of corrugated chains, implying an unoptimized production rate of $>10^5$ particles/h/cm^2. This estimate implies the simultaneous operation of 10−100 channels in a single device. For monolithic channels, this degree of parallelization is consistent with current microfluidic technology.[24] Thus, quantities necessary for applications such as 3D visualization of self-assembly or cell population barcoding are accessible by means of this technique.

Experimental Section

Materials. Polystyrene microspheres were used as precursors. The manufacturer reported diameter of the large and small spheres is 21.14 ± 0.04 μm and 9.91 ± 0.73 μm, respectively. The small particles contain a dye to distinguish them. In addition, for Figure 3G and H, production was performed with FITC-labeled, carboxyl-modified polystyrene spheres of diameter 3.0 ± 0.13 μm. The carrier solvent dimethyl sulfoxide (DMSO, Sigma-Aldrich) was selected because of its high boiling temperature (189 °C) and its nonswelling interaction with polystyrene ($\chi_{PS/DMSO} = 1.36$ at 25 °C and 1.20 at 80 °C).[25]

Microfabricated Device. Fluidic channels and metal heater were fabricated on opposite sides of a polished silicon oxide wafer (450 μm thickness, 100 mm diameter, 5000 Å thermal oxide layer). For channel etching, photoresist (PR 1827) was spun, patterned, and developed in MF 319 solution. The oxide layer of the developed region was etched in buffered hydrofluoric acid solution. Channels were etched in a STS Deep reactive ion etcher. After etching, the oxide layer on the channel side was again stripped. Metal heaters were fabricated on the backside by lift-off of a Ti/Pt (300 Å/1000 Å) layer in acetone solution. Ports for sample injection and fluidic control were made by electrochemical discharge drilling of a glass wafer (Pyrex 7740, 100 mm diameter, 700 μm thickness) that had been cleaned in hydrogen peroxide/sulfuric acid mixture (1:3 v/v). The resulting glass and silicon wafers were aligned, anodically bonded, diced, and wired to a printed circuit board. The production of anisotropic particles from 3.0-μm spheres was accomplished in a fluidic device stamped in poly(dimethyl siloxane) (PDMS, Sylgard 184 elastomer kit, Ellswoth Adhesive, WI) from a master generated on a silicon wafer with SU-8 2007 photoresist (Microchem Corp, MA). The photoresist was spun at 2000 rpm for 30 s to obtain a thickness of 8.5 μm, and the mask had a minimum channel dimension of 2 μm. The PDMS replica was sealed to a glass cover slip by UV/ozone treatment.

Fluidic Control. A software-configured pressure, vacuum, or neutral load was applied through syringes connected to each port. To rapidly switch ($t_{switch} \approx 5$ ms) between the three states during a production cycle, syringes were connected to a set of two-way and three-way solenoid valves (Numatech) that were operated by computer control (Labview 7.1, National Instruments).

Particle Fusing. Fusing is accomplished at a temperature set by controlling a Ti/Pt heater fabricated on the back of the chip. The resistance value of the metal heater is ∼0.39 kΩ. Fusing is accomplished by raising the temperature to a set point that can be varied between $T = 65-85$ °C. At the condition of 50 VDC ($T = 80$ °C) fusing is achieved in less than 300 ms. After heating, the particle is cooled by convective flow and then released into the collection chamber. For anisotropic particles synthesized from 3-μm precursor spheres, fusing was accomplished by illumination with a radiative source (50 W of duration = 10 s).

Image Acquisition and Processing. In situ imaging of the particles in the device was accomplished with a stereoscope (Olympus SZX-12) and digital camera (Nikon Coolpix 4500). High-resolution particle images were acquired with 10×, 40×, and 60× objectives on upright (Zeiss Axioscope) or inverted (Nikon Eclipse TE2000-U) microscopes. Bond angles between the fused particles were measured in the following way: The edge detection tool of image analysis software (ImageJ 1.34s, National Institutes of Health) was used to find particle boundaries. Particle centroids were determined from particle boundaries. The bond angle relative to the particle's central axis was determined from the centroid locations.

Acknowledgment. We acknowledge helpful discussions with S. C. Glotzer and N. A Kotov and the participation of Zachary Zell in experiments. This study was supported by NSF CBET 0507839.

JA0762700

(24) Thorsen, T.; Maerki, S. J.; Quake, S. R. *Science* **2002**, *298*, 580−584.
(25) Cong, Y.; Zhang, Z.; Fu, J.; Li, J.; Han, Y. *Polymer* **2005**, *46*, 5377−5384.